Environmental Science and Pollution Research (2019) 26:1315–1322
https://doi.org/10.1007/s11356-018-3652-0

RESEARCH ARTICLE

Removal of Pb(II) from aqueous solutions by adsorption on magnetic bentonite

Chenglong Zou[1] · Wei Jiang[1] · Jiyan Liang[1] · Xiaohang Sun[2] · Yinyan Guan[1]

Received: 28 July 2018 / Accepted: 31 October 2018 / Published online: 13 November 2018

Abstract

Bentonite is a porous clay material that shows good performance for adsorbing heavy metals and other pollutants for wastewater remediation. In our previous study, magnetic bentonite (M-B) was prepared to solve the separation problem and improve the operability. In this study, we investigated the influence of various parameters on the Pb(II) adsorption of M-B, and it showed effective performance. About 98.9% adsorption removal rate was achieved within 90 min at adsorbent dose of 10 g/L for initial Pb(II) concentration of 200 mg/L at 40 °C and pH 5. The adsorption kinetic fit well by the pseudo-second-order model, and also followed the intra-particle diffusion model up to 90 min. Moreover, adsorption data were successfully reproduced by the Langmuir isotherm; the maximum adsorption capacity was calculated as 80.40 mg/g. The mechanism of interaction between Pb(II) ions and M-B was ionic exchange, surface complexation, and electro-static interactions. Thermodynamics study indicated that the reaction of Pb(II) adsorption on M-B was endothermic and spontaneous; increasing the temperature promoted adsorption. This study was expected to provide a reference and theoretical basis for the treatment of Pb-containing wastewater using bentonite materials.

Keywords Bentonite · Magnetic · Pb(II) ions · Adsorption · Kinetics · Thermodynamics · Isotherms · Mechanism

Introduction

With the rapid development of industry, excessive heavy metals flowing into the environment will result in serious environmental pollution. Lead is a common contaminant found in wastewater and can come from many sources, such as metallurgy, electroplating, manufacturing and recycling of batteries, and the production of pigments and ammunition (Tunali et al. 2006). Lead is toxic, non-biodegradable, and can bio-accumulate in living cells (Ghorai et al. 2014). It can enter the human body through inhalation, ingestion, or skin contact and mainly accumulates in the bones, brain, kidney, and muscles, which may cause anorexia, loss of appetite, anemia, and long-term damage to the nervous and hematopoietic system, and even death (Kul and Koyuncu 2010; Farooq et al. 2010). Hence, lead is the primary pollutant that is monitored and controlled in all countries.

At present, common treatment methods for lead-containing wastewater include chemical precipitation, membrane filtration, electrolytic reduction, solvent extraction, adsorption, and ion exchange (Fu and Wang 2011). Among these methods, adsorption is highly effective, convenient, and economical. Bentonite clay is a beneficial adsorbent material for the treatment of environmental pollution due to its large surface area, high adsorption capacity, and low cost (Pan et al. 2011). However, bentonite is difficult to separate from wastewater after it has adsorbed the contaminant as it forms a stable dispersion. Previously, granulated bentonite materials were prepared to solve this separation problem; however, their adsorption capacity seems not to be very high (Cao et al. 2007;

Responsible editor: Tito Roberto Cadaval Jr

Electronic supplementary material The online version of this article (https://doi.org/10.1007/s11356-018-3652-0) contains supplementary material, which is available to authorized users.

✉ Jiyan Liang
liangjiy2017@126.com

[1] School of Science, Shenyang University of Technology, Shenyang 110870, Liaoning, China

[2] Department of Advanced Engineering, Muroran Institute of Technology, Muroran, Hokkaido 050-8585, Japan

Mo et al. 2017). Deposing magnetic Fe_3O_4 particles onto the surfaces of adsorbent powder can allow effective separation from wastewater using magnetic separation techniques (Chen et al. 2012; Jin et al. 2016).

In our study, magnetic bentonite (M-B) was prepared using the solvothermal method, aimed at developing a new low-cost adsorption material for treating heavy metal ions. The chemical composition, skeleton, structure surface morphology, and zeta potential of M-B have previously been analyzed using a range of instrumental techniques in our previous study (Zou et al. 2018). The main objective of the present investigation was to study the adsorption performance of M-B to Pb(II) for potential industrial applications. The effects of various parameters, including the contact time, pH, temperature, initial Pb(II) concentration, and dose of adsorbent on the adsorption performance, were considered through batch experiments. The results showed that the M-B has significant effect on the treatment for Pb(II) ions. Moreover, the mass transfer mechanisms and action mechanisms of adsorption Pb(II) from aqueous solutions onto M-B were studied using various kinetics, isotherms, and thermodynamics models. This study was expected to provide technical supports for promoting wider applications of bentonite as adsorbent materials.

Materials and methods

Materials and chemical reagents

Sodium bentonite (Na-B) was obtained from Chaoyang City (Liaoning province, China). The material was crushed and passed through a 200-mesh sieve after purification and air drying. The Na-B was a light yellow color. Analytical grade chemical reagents were used, including $FeCl_3{\cdot}6H_2O$, $FeSO_4{\cdot}7H_2O$, $AlCl_3{\cdot}6H_2O$, CH_3COONa, $(CH_2OH)_2$, NaOH, HNO_3, and $Pb(NO_3)_2$, which were purchased from Sinopharm Chemical Reagent Co. Ltd. (China). All solutions were prepared with deionized water.

Preparation of magnetic bentonite

The magnetic bentonite (M-B) was prepared through two main modification stages with reference to our previous study (Zou et al. 2018). The first stage was modifying sodium bentonite (Na-B) to aluminum-pillared bentonite (Al-B) using a modified method based on a recent report (Gu et al. 2011) where a ratio of aluminum to Na-B of 6 mol/kg was used. The second stage was modifying aluminum-pillared bentonite (Al-B) to magnetic bentonite (M-B) by depositing Fe_3O_4 magnetic particles onto the surfaces of Al-B using a previously reported solvothermal method (Lian et al. 2014); the ratio of iron to Al-B was 6 mol/kg.

Batch adsorption experiment

Simulated lead-containing wastewater was prepared by dissolving $Pb(NO_3)_2$ in deionized water. Batch experiments were carried out in a thermostatic water bath oscillator at 170 rpm. Two hundred microliters of simulated wastewater and the M-B adsorbent were added to a 500-ml conical flask. The pH was adjusted using 0.01 mol/L HNO_3 and 0.01 mol/L NaOH solutions. After absorption reaction, the adsorbent was separated using an external magnet. All experiments were conducted using three replicates. To examine the effects of various process variables on Pb(II) adsorption, the following experiments were performed:

1. Contact time: initial Pb(II) concentration of 200 mg/L, 10 g/L of M-B, temperature $T = 35$ °C, pH 5, and contact times 5, 10, 15, 20, 30, 45, 60, 75, and 90 min.
2. Temperature: initial Pb(II) concentration of 200 mg/L, 10 g/L of M-B, 10–50 °C, pH 5, and contact time 120 min.
3. pH: initial Pb(II) concentration 200 mg/L, 10 g/L of M-B, 35 °C, pH 2.0–6.5, and contact time 120 min.
4. Adsorbent: initial Pb(II) concentration 200 mg/L, 2.5–15.0 g/L of M-B, 35 °C, pH 5, and contact time 120 min.
5. Initial Pb(II) concentration: initial Pb(II) concentrations 50–400 mg/L, 10 g/L of M-B, 35 °C, pH 5, and contact time 120 min.

The Pb(II) concentration was analyzed using an AAS novAA 400 flame atomic absorption spectrophotometer (Analytik Jena AG, Germany).

Data processing

The removal rate (r, %) was determined using Eq. (1):

$$r = \frac{c_0 - c_e}{c_0} \times 100 \quad (1)$$

The adsorption amount (the amount of Pb(II) ions adsorbed per gram of M-B) (mg/g) was calculated using Eq. (2):

$$q_t = \frac{(c_0 - c_t) \times V}{M} \quad (2)$$

where c_0 is the initial Pb(II) concentration (mg/L), c_e is the Pb(II) concentration at equilibrium (mg/L), c_t is the Pb(II) concentration at time t (mg/L), V is the total volume of the solution (L), M is the mass of the M-B used (g), r is the removal rate (%), and q_t and q_e are the amounts of Pb(II) adsorbed per unit mass of M-B (mg/g) at time t and at equilibrium, respectively.

Results and discussion

Effect of contact time and adsorption kinetics

First, the effect of the contact time was studied. The plot (see in Fig. 1a) showed adsorption kinetics of Pb(II) on M-B consisted of two phases: an initial rapid phase and a second slower phase. The first phase showed a rapid uptake of Pb(II) onto the M-B during the first 15 min. The removal rate increased gradually with increasing contact time. The equilibrium uptake was achieved at ~90–120 min. Further increased of contact time did not result in removal rate, and Pb(II) removal for a concentration of 200 mg/L reached 98.76%. Thus, to ensure maximum Pb(II) ion removal, 120 min has been selected as optimum contact time in the following experiments.

In order to further explore the rate-controlling steps during adsorption and the dynamic characteristics of the adsorption process, the Lagergren pseudo-first order and pseudo-second order kinetic models were applied to the experimental data; the kinetic equations are shown in Eq. (3) and Eq. (4), respectively (Monfared et al. 2015). In order to describe the localized adsorption for specific interactions, the intra-particle diffusion model proposed by Weber and Morris was applied to analyze the adsorption process, as expressed by Eq. (5) (Mohseni-Bandpi et al. 2016).

$$q_t = q_e\left(1-e^{-k_1 t}\right) \tag{3}$$

$$q_t = \frac{k_2 q_e^2 t}{1 + k_2 q_e t} \tag{4}$$

$$q_t = k_3 t^{0.5} + C \tag{5}$$

where k_1, k_2, and k_3 are the rate constants of the pseudo-first order (min^{-1}), pseudo-second order (g/(mg min)) adsorption equations, and the intra-particle diffusion model (mg/(g $min^{0.5}$)), respectively. C is the intercept, which is related to the boundary layer thickness (mg/g).

The plots of the nonlinear form of the kinetic models are shown in Fig. 1b. The adsorption and rate constants calculated from the plots are shown in Table 1. The correlation coefficient R^2 of the pseudo-second-order model was larger, and q_e values calculated using the pseudo-second order equations were closer to those determined experimentally. The kinetic data showed a better fit to the pseudo-second-order kinetic model, suggesting the occurrence of chemical adsorption.

The intra-particle diffusion model was used to analyze the rate-controlling step of the adsorption reaction. The fitting results indicated that the adsorption of Pb(II) onto M-B may be followed by the model up to 90 min. The plots (Fig. 1b) present two distinct adsorption stages, and the mass transfer rate in the initial and final stages of adsorption was different, indicating the surface adsorption and intra-particle diffusion concurrently operating during the interactions of Pb(II) and M-B. The first sharper portion stage was attributed to the diffusion of Pb(II) ions through the solution to the external surface of M-B and adsorption on active sites of the M-B surface (surface adsorption process); the adsorption rate mainly was influenced and controlled by the liquid film diffusion. While the second gradual stage was attributed to diffusion of Pb(II) ions in the pores of M-B and absorption in the pores (particle diffusion process), the adsorption rate mainly was influenced and controlled by the intra-particle diffusion. As shown in Table 1, the two intercepts C of the two distinct particle diffusion processes were not equal to zero. This indicated that the intra-particle diffusion was not the only rate-controlling step but some degree of the boundary layer diffusion also controlled the adsorption (Kang et al. 2009), which was consistent with the analysis of pseudo-second-order kinetics.

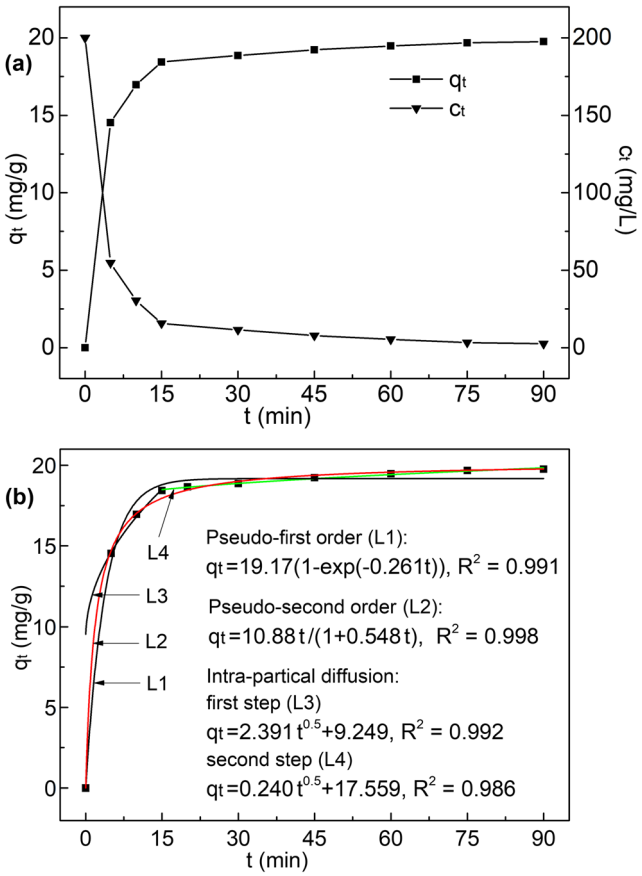

Fig. 1 **a** Effect of contact time on q_t and c_t. **b** Pseudo-first-order, pseudo-second-order, and intra-particle diffusion kinetic models for Pb(II) adsorption onto M-B

Effect of temperature and adsorption thermodynamics

The effect of temperature on the adsorption of Pb(II) by M-B was analyzed as the reaction temperature is known to affect the adsorption efficiency (Daou et al. 2017). The temperature dependence of both equilibrium concentration (c_e) and removal rate (r) is shown in Fig. 2a. The removal rate increased

Table 1 Kinetic parameters for adsorption of Pb(II) onto M-B

Pseudo-first order		Pseudo-second order		Intra-particle diffusion		
$q_{e,\ exp}$ (mg/g)	19.74	$q_{e,\ exp}$ (mg/g)	19.74	–	First step	Second step
$q_{e,\ cal}$ (mg/g)	19.17	$q_{e,\ cal}$ (mg/g)	19.86	C	9.249	17.559
k_1 (min^{-1})	0.261	k_2 (g/(mg min))	0.0276	k_3 (mg/(g $min^{0.5}$))	2.391	0.240
R^2	0.991	R^2	0.998	R^2	0.992	0.986

slightly from 92.0 to 98.9% with a temperature increased from 10 to 40 °C. The equilibrium adsorption quantity was 19.79 mg/g, and the residual concentration of Pb(II) was 2.15 mg/L at 40 °C. The adsorption amount decreased slightly above 40 °C. This is because increasing the temperature promotes mass transfer, which is beneficial for adsorption. However, higher temperatures are not conducive to ion covalent bonds. In general, the reaction temperature had little influence on the efficiency of adsorption. This was consistent with the results of a previous report (Yi et al. 2015).

The adsorption process was further analyzed using thermodynamic analyses. Thermodynamic parameters, such as the changes in the Gibbs free energy (ΔG), enthalpy (ΔH), and entropy (ΔS), depend on the adsorption process and were determined using the following Eqs. (6–10) (Yao et al. 2014). In the determination of thermodynamic, the K_d value should be dimensionless by multiplying K_e by the density of the liquid (Milonjic 2007; Frantz Jr et al. 2017).

$$K_e = \frac{q_e}{c_e} \tag{6}$$

$$K_d = K_e \times \rho_w \tag{7}$$

$$\Delta G = -RTlnK_d \tag{8}$$

$$\Delta G = \Delta H - T\Delta S \tag{9}$$

$$lnK_d = \frac{\Delta S}{R} - \frac{\Delta H}{RT} \tag{10}$$

where K_e is the ratio of the adsorption capacity at equilibrium (L/g), ρ_w is the density of the water (1000 g/L), and K_d is the adsorption equilibrium constant.

The adsorption results between 10 and 40 °C were studied. The plot of $\ln K_d$ versus $1/T$ is shown in Fig. 2b; the values of thermodynamic parameters ΔH, ΔS, and ΔG obtained are listed in Table 2. The value of $\Delta H = 51.23$ kJ/mol indicated that the Pb(II) adsorption was an endothermic process; the ΔH value exceeded 40 kJ/mol indicated that the adsorption of Pb(II) onto M-B was chemical adsorption. The value of $\Delta S = 239.2$ J/(mol·K) suggested an increase in randomness at the solid–liquid interface during the adsorption process and reflected the affinity of M-B for Pb(II) ions (Yao et al. 2014). The ΔG values decreased from − 16.46 to − 23.64 kJ/mol when the temperature was increased from 283 to 313 K, which indicated the adsorption processes were spontaneous in nature. Furthermore, the decrease in ΔG values with increasing temperatures suggested that the adsorption was more favorable at higher temperatures for temperatures below 313 K (Moussout et al. 2016).

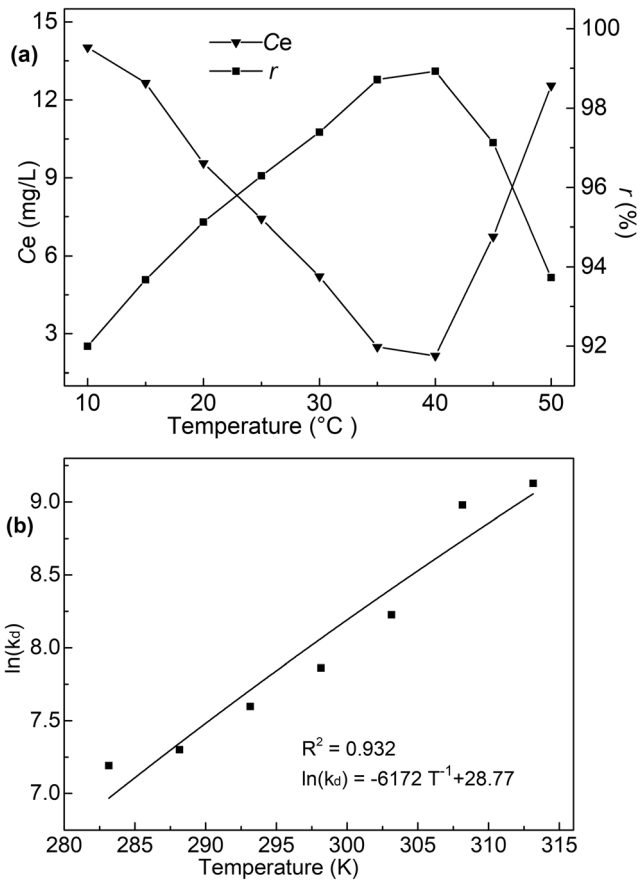

Fig. 2 **a** Effect of temperature on the equilibrium concentration (c_e) and removal rate (r). **b** The Van't Hoff plot of $\ln K_d$ versus T

Table 2 Thermodynamic parameters of Pb(II) adsorption onto M-B

T (K)	ΔG (kJ/mol)	ΔH (kJ/mol)	ΔS (J/(mol K))
283	− 16.46	51.27	239.2
288	− 17.66		
293	− 18.85		
298	− 20.05		
303	− 21.24		
308	− 22.44		
313	− 23.64		

Effect of pH

The pH of a solution is the most influential parameter determining metal adsorption as it greatly affects the surface charge of the adsorbent and the speciation of the metals in solution (Liu et al. 2013). It is generally considered that acidic conditions are unfavorable for the adsorption of heavy metal ions by bentonite, while neutral and alkaline conditions are favorable (Shi and Liu 2006). Hence, it is necessary to study the effect of pH on the adsorption process (Shi et al. 2016). The effect of pH on the adsorption of Pb(II) by M-B was analyzed, where the pH dependence of both equilibrium concentration (c_e) and removal rate (r) is shown in Fig. 3.

As shown in Fig. 3, the adsorption removal of Pb(II) was significantly affected by pH. Increasing the pH resulted in a rapid and continuous decrease in c_e. With increasing pH, r steadily increased up to a pH of 5 to reach 98.72%. The equilibrium adsorption capacity increased with increasing pH and was 19.74 mg/g at pH 5.0. Further increasing the pH resulted in a little increase in r. When the pH was 6.5, the removal rate reached 99.52%. The above results might be due to the several following reasons. As the zeta potential measurements shown in Supplementary Fig. 3, the point of zero charge (PZC) of M-B corresponded to pH 3.6. At low pH, M-B exhibited positive zeta potentials with the positively charged surface; Pb(II) ions in the solution were repelled by the positively charged M-B surface. Additionally, there are many H_3O^+ ions in solution at low pH which competed with Pb(II) for adsorption sites, effectively decreasing the adsorption of positively charged ions (Blázquez et al. 2012). At high pH, M-B exhibited negative zeta potentials and decreased with the increase of pH, indicating the number of metal-binding sites on the negatively charged sites increased. As a result, the Pb(II) adsorption capacity of M-B increased owing to the electro-static attraction between Pb(II) ions and the negatively charged M-B surface. Furthermore, the adsorption of Pb(II) increased as Pb(II) ions will combine with OH^- ions to form precipitates under these conditions (Singanan 2011). Similar findings were previously reported for metal adsorption using various adsorbents (Singanan 2011).

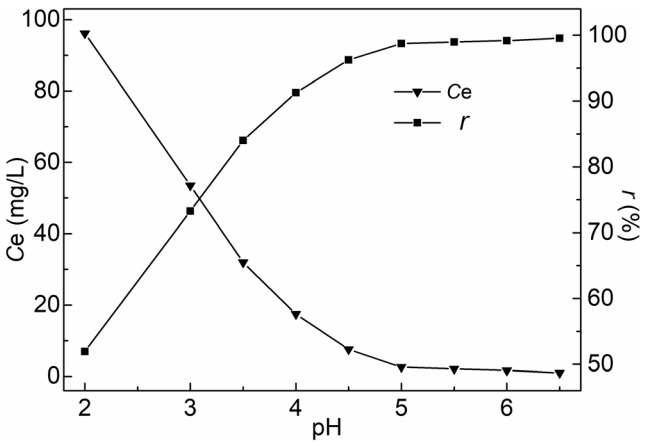

Fig. 3 Effect of pH on the equilibrium concentration (c_e) and removal rate (r) of M-B

Effect of adsorbent

The adsorption efficiency was affected by both the saturated adsorption capacity and the balance between ions in the two phases. Therefore, the type of adsorbent used influences the adsorption efficiency. The effects of the adsorbent type and adsorbent dose on equilibrium absorption amount (q_e) and removal rate (r) are shown in Fig. 4.

The adsorption efficiency of M-B was clearly higher than that of Na-B, indicating that the adsorption performance was enhanced after modification. It may be due to several reasons below: As the characterizations of specific surface area and pore properties shown in Supplementary Table 1, the specific surface area and the total pore volume of M-B increased after modification, improving the adsorption sites on the surface. And the pore size of M-B increased, which was beneficial for Pb(II) ion diffusion into pore, increasing the utilization of adsorption sites on the pore surface significantly. The zeta

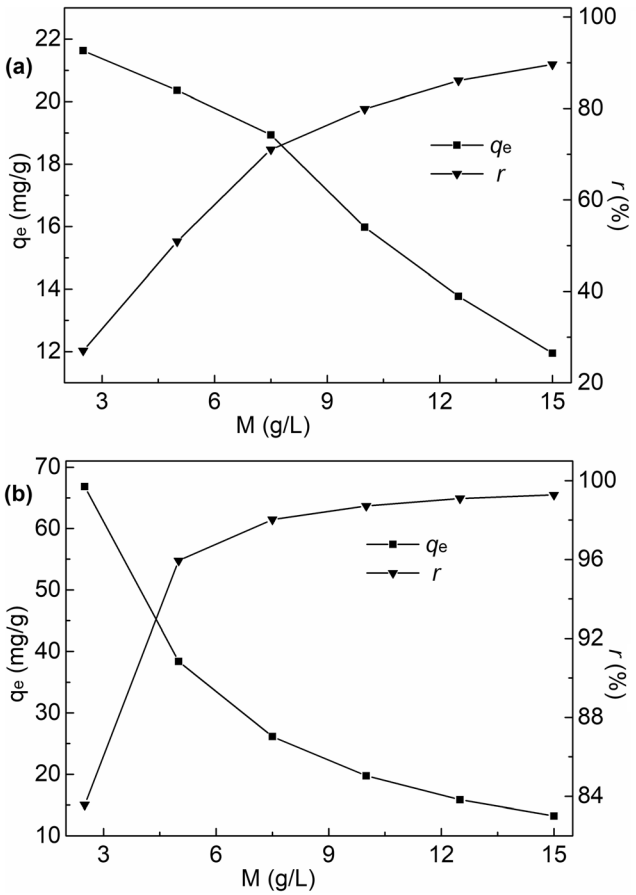

Fig. 4 Effect of adsorbent dose on the equilibrium absorption amount (q_e) and removal rate (r) of Na-B (**a**) and M-B (**b**)

potential of M-B was lower than that of Na-B at pH 5.0, indicating more metal-binding sites with the negatively charged sites and showing stronger electro-static attraction for Pb(II). In the weak acid solution, some Al_2O_3 and Fe_3O_4 loaded on the M-B became high flocculation adsorption activity sites on the surface of M-B. Moreover, some Al_2O_3 and Fe_3O_4 became cations, which increased the number of exchangeable cations on the M-B.

The removal rate of Pb(II) increased with increasing M-B dose from 2.5 to 10.0 g/L, which was simply due to the increasing number of adsorption sites (Singanan 2011). Further increasing the M-B dose had a negligible effect on the removal rate, attributed to an insufficient residual metal concentration in solution (Hamane et al. 2015). In addition, the adsorption process should follow isothermal adsorption equilibrium theory. Up to an M-B dose of 20 g/L, the residual Pb(II) concentration in solution was lower than 1.00 mg/L, which satisfies the integrated wastewater discharge standard of China (GB 8978-1996). When the M-B dose was increased, the removal rate (r) of Pb(II) increased while the equilibrium adsorption amount (q_e) decreased. It may be due to several reasons below: Increased of M-B dose can be attributed to aggregation of adsorbent particles, which decreased total surface area of the adsorbent and increased diffusional path length (Shukla et al. 2002). With further increased in the dose of the M-B, the aggregation became increasingly significant, causing a decrease in active sites and hence decreased in adsorption. Secondly, at constant volume of adsorbate, the solid/liquid ratio increased which left many sites unoccupied during adsorption process and hence a reduction in the adsorption capacity of the adsorbent (Olu-Owolabi et al. 2010). Moreover, the equilibrium absorption amount (q_e) is mainly affected by the adsorption capacity of adsorbent and the concentration of Pb(II) in aqueous solution. The adsorption process should follow isothermal adsorption equilibrium theory. As the dose of M-B increased, the amount of Pb(II) absorbed on M-B increased, i.e., the amount of Pb(II) remaining in the solution decreased, which decreased the driving force for mass transfer between the aqueous and solid phases provided by the Pb(II) concentration and hence decreased in adsorption.

Effect of initial Pb(II) concentration

The main mechanism of heavy metal ion adsorption on bentonite is related to ion exchange. The ion exchange capacity is mainly affected by the cation exchange capacity of bentonite and the concentration of heavy metal ions in aqueous solution. Increasing the heavy metal ion concentration can improve the exchange capacity. In addition, the initial concentration provides a driving force for mass transfer between the aqueous and solid phases (Oubagaranadin et al. 2010). The effects of different initial Pb(II) concentrations on equilibrium absorption amount (q_e) and removal rate (r) are shown in Fig. 5.

With the initial Pb(II) concentration increased from 50 to 400 mg/L, the adsorption amount of Pb(II) ions increased from 4.95 to 39.26 mg/g. The r decreased slightly over the measured concentration range; this may be due to the equilibrium adsorption quantity being far from the saturated adsorption capacity. Only when the initial concentration was < 100 mg/L did the residual Pb(II) concentration fall below the wastewater discharge limit of 1.00 mg/L (GB 8978-1996). The preparation of magnetic bentonite with strong adsorption ability was demonstrated. However, it was difficult to achieve the Pb(II) concentration limit for high-concentration wastewater only once using continuous stirred method. If it was used for the pretreatment of high-concentration Pb(II) wastewater, M-B would adsorb most of the Pb(II) ions. In addition, if it was used in a multilevel series operation mode, M-B could reduce the residual Pb(II) ion concentration below the limit required by the standard.

In order to further clarify the adsorption mechanism, we investigated the relationship between the Pb(II) adsorbed per gram of M-B and the equilibrium concentration. The adsorption process was analyzed using the Langmuir and Freundlich adsorption isotherms (Shah et al. 2017; Kameda et al. 2018). The adsorption isotherm equations are shown as Eq. (11) and Eq. (12).

$$\text{Langmuir}: q_e = Q\frac{K_L C_e}{1 + K_L C_e} \tag{11}$$

$$\text{Freundlich}: q_e = K_F C_e^{1/n} \tag{12}$$

where Q is the Langmuir monolayer adsorption capacity (mg/g), the Pb(II) content required to occupy all the available sites for a unit mass of M-B (mg/g); and K_L is the Langmuir constant (L/g). K_F and n are the Freundlich constants referring to the adsorption capacity and the adsorption intensity, respectively.

The equilibrium data (amounts of Pb(II) adsorbed per gram of M-B and the equilibrium concentrations of Pb(II)) were fitted using isotherms. The plots of the nonlinear form of the

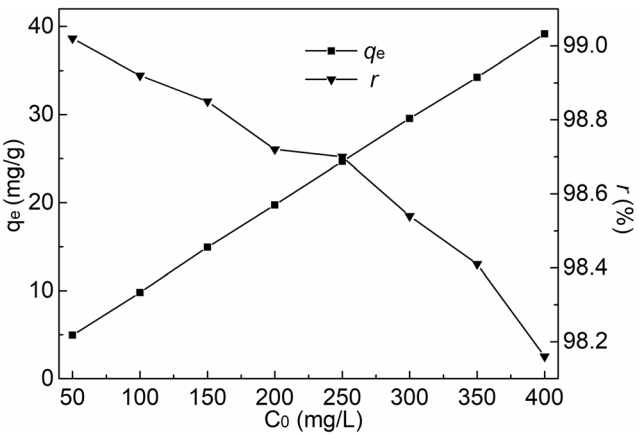

Fig. 5 Effect of initial Pb(II) concentration on the equilibrium absorption amount (q_e) and removal rate (r) of M-B

adsorption isotherm models are shown in Fig. 6, and the constants obtain from plots were shown in Table 3. The R^2 value of the Langmuir model was larger than that of the Freundlich model; therefore, the Langmuir isotherm equation can better describe the adsorption behavior of Pb(II) on M-B and indicated it was a monolayer adsorption reaction. In addition, the adsorption saturation capacity of M-B was calculated as 80.40 mg/g. The fractional value of $1/n = 0.689$ ($0 < 1/n < 1$) indicated a heterogeneous surface structure of the material with an exponential distribution of active sites. In addition, a strong affinity of M-B toward Pb(II) ions was indicated by the higher values of the Freundlich adsorption capacity obtained.

The essential characteristics of the Langmuir isotherm can be expressed by a dimensionless constant called the equilibrium parameter (R_L), as defined by the following Eq. (13) (Yao et al. 2014):

$$R_L = \frac{1}{1 + k_L C_0} \tag{13}$$

The R_L value indicates the nature of the isotherm: irreversible ($R_L = 0$), favorable ($0 < R_L < 1$), linear ($R_L = 1$), or unfavorable ($R_L > 1$) (Kang et al. 2009). The K_L value calculated from the plot was 0.132 L/mg. When the initial Pb(II) concentration increased from 50 to 400 mg/L, the calculated R_L values ranged from 0.132 to 0.0186, indicating a favorable adsorption.

Additionally, the adsorption mechanism can be deduced from the average adsorption free energy (*Es*) calculated using the Dubinin-Radushkevich (D-R) adsorption isotherm model (Eqs. (14–16)) (Chen et al. 2017):

$$q_e = q_m \times e^{\left(-k_d \varepsilon^2\right)} \tag{14}$$

$$\varepsilon = RT \ln\left(1 + \frac{1}{c_{e2}}\right) \tag{15}$$

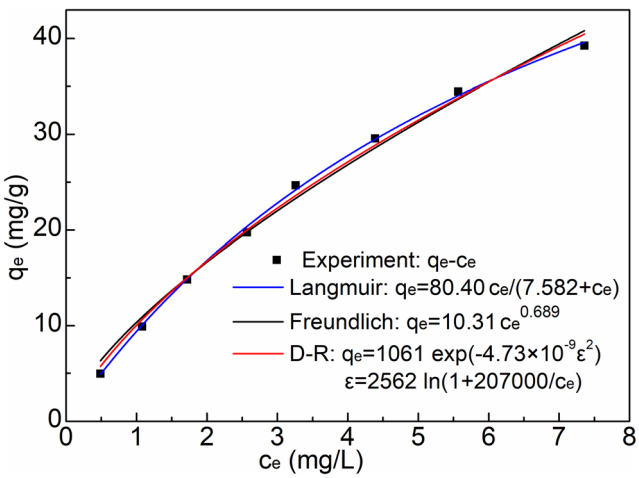

Fig. 6 The Langmuir, Freundlich, and D-R isotherm models for Pb(II) adsorption onto M-B

Table 3 Parameters of the Langmuir, Freundlich, and D-R isotherm models

Langmuir		Freundlich		D-R	
K_L (L/mg)	0.132	K_F	10.31	q_m (mg/g)	1061
Q (mg/g)	80.40	n	1.451	Es (kJ/mol)	10.28
R^2	0.995	R^2	0.990	R^2	0.993

$$E_s = \frac{1}{\sqrt{2k_d}} \tag{16}$$

where q_m is the maximal adsorption capacity (mg/g), c_{e2} is the Pb(II) concentration at equilibrium (mol/L), k_d is a constant (mol^2/J^2), T is the temperature (K), R is the universal gas constant (8.3145 J/(mol·K)), and ε is the Polanyi potential (J/mol).

The fits obtained using the nonlinear equation of D-R model are shown in Fig. 6. As shown in Table 3, q_m value calculated from the D-R model was significantly larger than Q value calculated from the Langmuir model. This was because the Langmuir model is based on mono molecule layer adsorption; adsorption only occurs on the outer surface of the adsorbent, while D-R model is based on the assumption of the adsorbent pores filling with solute (Cantuaria et al. 2015; D'Arcy et al. 2011). Based on the obtained k_d value, *Es* was calculated as 10.28 kJ/mol according to Eq. (16). The fact that this value was in the range of 8–16 kJ/mol indicated the occurrence of ionic exchange, surface complexation, and electro-static interactions during adsorption; the adsorption process was controlled by a chemical mechanism (Daneshvar et al. 2012; Hu et al. 2011).

Conclusions

The prepared M-B showed effective performance on Pb(II) adsorption. At 40 °C and pH 5.0, adsorption in an initial concentration of 200 mg/L Pb(II) ions with 10 g/L of M-B, the equilibrium adsorption quantity was 19.79 mg/L; the residual concentration of Pb(II) ions was 2.15 mg/L, and the adsorption removal rate reached 98.9%. The adsorption process of Pb(II) ions on M-B fit well by a pseudo-second-order model, and also followed the intra-particle diffusion model up to 90 min. Moreover, adsorption data were successfully described by the Langmuir model, and the adsorption saturation capacity of Pb(II) calculated as 80.40 mg/g. The adsorption data were well fitted with D-R isotherm model, and the average adsorption free energy change calculated was 10.28 kJ/mol, indicating the adsorption process mainly corresponded to ionic exchange, surface complexation, and electro-static interactions. Overall, the thermodynamic parameters implied that the endothermic adsorption process occurred spontaneously, and increasing the temperature promoted adsorption.

Funding information The authors are grateful for financial support from "Liaoning BaiQianWan Talents Program" and the China Environmental Protection Foundation, Geping Green Action, "123 Project" (Grant No. CEPF2014-123-1-6).

References

Blázquez G, Martín-Lara MA, Dionisio-Ruiz E, Tenorio G, Calero M (2012) Copper biosorption by pine cone shell and thermal decomposition study of the exhausted biosorbent. J Ind Eng Chem 18(5): 1741–1750

Cantuaria ML, Neto AFDA, Nascimento ES, Vieira MGA (2015) Adsorption of silver from aqueous solution onto pre-treated bentonite clay: complete batch system evaluation. J Clean Prod 112:1112–1121

Cao JL, Chen XQ, Liu XW, Tan ZY, An LJ, Zhang K (2007) Preparation and application of magnetic bentonite clean water reagent. J Tianjin Univ 40(4):457–462

Chen L, Yu S, Huang L, Wang G (2012) Impact of environmental conditions on the removal of Ni (II) from aqueous solution to bentonite/iron oxide magnetic composites. J Radioanal Nucl Chem 292(3): 1181–1191

Chen YG, Sun Z, Ye WM, Cui YJ (2017) Adsorptive removal of Eu(III) from simulated groundwater by GMZ bentonite on the repository conditions. J Radioanal Nucl Chem 311:1839–1847

Daneshvar E, Kousha M, Jokar M, Koutahzadeh N, Guibal E (2012) Acidic dye biosorption onto marine brown macroalgae: isotherms, kinetic and thermodynamic studies. Chem Eng J 204–206(18):225–229

Daou I, Zegaoui O, Amachrouq A (2017) Study of the effect of an acid treatment of a natural Moroccan bentonite on its physicochemical and adsorption properties. Water Sci Technol 75(5):1098–1117

D'Arcy M, Weiss D, Bluck M, Vilar R (2011) Adsorption kinetics, capacity and mechanism of arsenate and phosphate on a bifunctional TiO_2-Fe_2O_3 bi-composite. J Colloid Interf Sci 364:205–212

Farooq U, Kozinski JA, Khan MA, Athar M (2010) Biosorption of heavy metal ions using wheat based biosorbents-a review of the recent literature. Bioresour Technol 101(14):5043–5053

Frantz TS Jr, N S, Quadro MS, Andreazza R, Barcelos AA Jr, C T, Pinto LAA (2017) Cu(II) adsorption from copper mine water by chitosan films and the matrix effects. Environ Sci Pollut Res 24(6):1–10

Fu F, Wang Q (2011) Removal of heavy metal ions from wastewaters: a review. J Environ Manag 92(3):407–418

Ghorai S, Sarkar AK, Pal S (2014) Rapid adsorptive removal of toxic Pb^{2+}, ion from aqueous solution using recyclable, biodegradable nanocomposite derived from templated partially hydrolyzed xanthan gum and nanosilica. Bioresour Technol 170(5):578–582

Gu L, Xu J, Lv L, Liu B, Zhang H, Yu X, Luo ZX (2011) Dissolved organic nitrogen (DON) adsorption by using Al–pillared bentonite. Desalina 269(1–3):206–213

Hamane D, Arous O, Kaouah F, Trari M, Kerdjoudj H, Bendjama Z (2015) Adsorption/ photo–electrodialysis combination system for Pb^{2+}, removal using bentonite/ membrane/ semiconductor. J Environ Chem Eng 3(1):60–69

Hu B, Luo H, Chen H, Dong T (2011) Adsorption of chromate and paranitrochlorobenzene on inorganic-organic montmorillonite. Appl Clay Sci 51(1–2):198–201

Jin MJ, Long MC, Su HR, Pan Y, Zhang QZ, Wang J, Zhou BX, Zhang YW (2016) Magnetically separable maghemite/montmorillonite composite as an efficient heterogeneous Fenton–like catalyst for phenol degradation. Environ Sci Pollut Res 24(2):1926–1937

Kameda T, Umetsu M, Kumagai S, Yoshioka T (2018) Equilibrium studies of the adsorption of aromatic disulfonates by Mg–Al oxide. J Physi Chem Sol 114:129–132

Kang Q, Zhou W, Li Q, Gao B, Fan J, Shen D (2009) Adsorption of anionic dyes on poly(epicholorohydrin dimethylamine) modified bentonite in single and mixed dye solutions. Appl Clay Sci 45(4): 280–287

Kul AR, Koyuncu H (2010) Adsorption of Pb(II) ions from aqueous solution by native and activated bentonite: kinetic, equilibrium and thermodynamic study. J Hazard Mater 179(1):332–339

Lian L, Cao X, Wu Y, Sun D, Lou D (2014) A green synthesis of magnetic bentonite material and its application for removal of microcystin-LR in water. Appl Surf Sci 289(8):245–251

Liu M, Hou LA, Xi B, Zhao Y, Xia X (2013) Synthesis, characterization, and mercury adsorption properties of hybrid mesoporous aluminosilicate sieve prepared with fly ash. Appl Surf Sci 273(100):706–716

Milonjic SK (2007) A consideration of the correct calculation of thermodynamic parameters of adsorption. J Serb Chem Soc 72(12):1363–1367

Mo W, He Q, Su X, Ma S, Feng J, He Z (2017) Preparation and characterization of a granular bentonite composite adsorbent and its application for Pb^{2+} adsorption. Appl Clay Sci 159(6):68–73

Mohseni-Bandpi A, Al-Musawi TJ, Ghahramani E, Zarrabi M, Mohebi S, Vahed SA (2016) Improvement of zeolite adsorption capacity for cephalexin by coating with magnetic Fe_3O_4 nanoparticles. J Mol Liq 218:615–624

Monfared AD, Ghazanfari MH, Jamialahmadi M, Helalizadeh A (2015) Adsorption of silica nanoparticles onto calcite: equilibrium, kinetic, thermodynamic and DLVO analysis. Chem Eng J 281(1):334–344

Moussout H, Ahlafi H, Aazza M, Zegaoui O, El AC (2016) Adsorption studies of Cu(II) onto biopolymer chitosan and its nanocomposite 5% bentonite/chitosan. Water Sci Technol 73(9):2199–2210

Olu-Owolabi BI, Popoola DB, Unuabonah EI (2010) Removal of Cu^{2+} and Cd^{2+} from aqueous solution by bentonite clay modified with binary mixture of goethite and humic acid. Water Air Soil Poll 211(1–4):459–474

Oubagaranadin JUK, Murthy ZVP, Mallapur VP (2010) Removal of Cu(II) and Zn(II) from industrial wastewater by acid-activated montmorillonite-illite type of clay. C R Chim 13(11):1359–1363

Pan DQ, Fan QH, Li P, Liu SP, Wu WS (2011) Sorption of Th(IV) on Na-bentonite: effects of pH, ionic strength, humic substances and temperature. Chem Eng J 172(2):898–905

Shah J, Jan MR, Muhammad M, Ara B, Fahmeeda F (2017) Kinetic and equilibrium profile of the adsorptive removal of acid red 17 dye by surfactant-modified fuller's earth. Water Sci Technol 75(6):1410–1420

Shi H S, Liu Y H (2006) Adsorption characteristics of bentonite to Pb^{2+}, Zn^{2+}, Cr(VI), Cd^{2+}. J Build Mater 9(5):507–510

Shi J, Zhao ZW, Liang ZJ, Sun TY (2016) Adsorption characteristics of Pb(II) from aqueous solutions onto a natural biosorbent, fallen arborvitae leaves. Water Sci Technol 73(10):2422–2429

Shukla A, Zhang YH, Dubey P, Margrave JL, Shukla SS (2002) The role of sawdust in the removal of unwanted materials from water. J Hazard Mater 95(1):137–152

Singanan M (2011) Removal of lead (II) and cadmium (II) ions from wastewater using activated biocarbon. Sci Asia 37115(37):115–119

Tunali S, Akar T, Özcan AS, Kiran I, Özcan A (2006) Equilibrium and kinetics of biosorption of lead (II) from aqueous solutions by Cephalosporium aphidicola. Sep Purif Technol 47(3):105–112

Yao QX, Xie JJ, Liu JX, Kang HM, Liu Y (2014) Adsorption of lead ions using a modified lignin hydrogel. J Poly Res 21(6):465

Yi ZJ, Yao J, Kuang YF, Chen HL, Wang F, Yuan ZM (2015) Removal of Pb(II) by adsorption onto Chinese walnut shell activated carbon. Water Sci Technol 72(6):983–989

Zou C, Liang J, Jiang W, Guan Y, Zhang Y (2018) Adsorption behavior of magnetic bentonite for removing (II) from aqueous solutions. RSC Adv 8(48):27587–27595